Reverse-Selective Diffusion in Nanocomposite Membranes

Reghan J. Hill*

Department of Chemical Engineering and McGill Institute for Advanced Materials, McGill University, Montreal, Quebec H3A 2B2, Canada

(Received 21 September 2005; published 30 May 2006)

The permeability of certain polymer membranes with impenetrable nanoinclusions increases with the particle volume fraction [T. C. Merkel *et al.*, Science **296**, 519 (2002)]. The discovery contradicts qualitative expectations based on Maxwell's classical theory of conduction or diffusion in composites with homogeneous phases. This Letter presents a theory based on an hypothesis that polymer chains are repelled from the inclusions during membrane casting. The accompanying increase in free volume, and hence solute diffusivity, yields bulk transport properties that are in good agreement with experiments.

DOI: 10.1103/PhysRevLett.96.216001 PACS numbers: 83.80.Ab

Polymeric membranes facilitate a variety of molecular separations. Because their microstructure is of molecular scale, the polymer architecture can be tailored to specific penetrant mixtures. Merkel *et al.* [1,2] recently showed that incorporating nanometer sized inorganic particulates into certain amorphous polymer glasses increases the membrane permeability and selectivity. Because of its significant technological applications, this discovery has stimulated further experimental investigations [3–6]. However, a theory that quantifies how the inclusion size and concentration affect the permeability and selectivity has yet to emerge.

Merkel *et al.* highlighted that classical Maxwell-like theories fail to describe the qualitative trends. More importantly, they pointed out that the Cohen-Turnbull free-volume theory [7] can be invoked to explain qualitative aspects of the enhanced permeability and reverse selectivity. Their idea is significantly extended in this Letter to achieve a quantitative interpretation of the experiments. The theory is based on classical Fickian diffusion past an impenetrable sphere (silica nanoinclusion) embedded in a polymeric continuum. A classical methodology is used to derive the effective diffusivity for a dilute random array of such inclusions. However, a thin layer at the inclusion-polymer interface is presumed to exist where the polymer segment density is lower than in the bulk. It is hypothesized that the accompanying increase in free volume reflects a repulsive interaction between the polymer chains and inclusions during membrane casting. The accompanying increase in the local diffusivity of a penetrant molecule is demonstrated to yield a bulk (diffusive) permeability enhancement that is commensurate with the experiments of Merkel *et al.*.

The assumption that polymer is depleted in the interfacial region is supported, in part, by experiments showing that the average *polymer* density in dry composite membranes decreases with increasing silica content [2]. Also, transmission electron microscopy images of silica-based nanocomposites [2] *suggest* particle aggregation. Note that quiescent solutions of polymer, silica, and solvent often phase separate, and surface modifications have a significant influence on dispersion stability and inclusion-polymer adhesion [2,8]. Indeed, the fumed silica in the experiments of Merkel *et al.* was chemically modified, making it compatible with the organic solvent that also hosts the polymer during membrane casting. In this work, an attractive interparticle potential is attributed to polymer depletion [9]. However, because of intense initial mixing, and an increasing bulk viscosity during casting (slowing microstructural dynamics), the final distribution is likely to reflect a ''snapshot'' of the relaxation toward equilibrium. Under these conditions, equilibrium is established on the polymer-chain length scale, simplifying the problem to one with polymer depletion at the surfaces of well dispersed (noninteracting) inclusions.

During evaporation, the polymeric phase is transformed from a dilute or semidilute solution, through a concentrated solution and melt, to an amorphous glass. Diffusion coefficients of high molecular weight polymers in semidilute solutions are in the range $D \sim 10^{-11}$–10^{-13} $m^2\,s^{-1}$ [10]. Therefore, the characteristic time for a polymer to diffuse (reptate) a distance comparable to its size, say, $l \sim 10$ nm, will be at most $\sim l^2/D \sim 10^{-3}$ s. Cast membranes are dried over a period of about 24 h [2], so, assuming the average polymer concentration remains uniform, chains have time to adopt equilibrium conformations. However, in the last stage of drying, which may be assumed to occur at constant polymer density (polymer volume fraction ≈ 0.8), the characteristic time for a uniform solvent front to traverse a polymer is ~ 0.1 s. Therefore, because chain mobility (and flexibility) decreases with increasing polymer volume fraction, it is not unreasonable to expect equilibrium conformations to be *frozen* into the (final) glassy state (rigid chains).

For steady gas permeation across a membrane with thickness L, the diffusive flux is

$$|\langle \boldsymbol{j} \rangle| = -D^e \Delta n / L, \tag{1}$$

where D^e is the effective diffusivity, and Δn is the differential concentration of the diffusing penetrant. In this

work, the gas solubility is assumed to be independent of the solids concentration, so the inclusions are assumed to influence the permeability only through their role in modifying the effective diffusivity D^e. This should be a reasonable approximation for the polymer composites and penetrants to which the model is compared. Merkel *et al.* showed that the solubilities of nitrogen and methane in poly(4-methyl-2-pentyne) (PMP)/silica composites are independent of the silica loading [2]. Similar conclusions were drawn for *n*-butane. For PMP/silica composites, which form the basis of the theoretical interpretation of experiments in this Letter, Merkel *et al.* conclude that permeability and selectivity are enhanced principally by changes in penetrant mobility. They also presented data showing that the most significant influence on the penetrant diffusivity comes from the silica loading, not the relatively small changes due to penetrant concentration.

Note that the experiments of Merkel *et al.* exhibit *reverse selectivity*, meaning that the permeability of larger molecules is enhanced more than smaller ones. They point out that this necessitates molecular-scale perturbations to the polymer microstructure, which precludes the notion that the permeability is enhanced by shells of void space, for example, between the (impenetrable) inclusions and surrounding polymer. Such voids are understood to give rise to Knudsen diffusion, which does not yield a reverse-selective increase in permeability. Rather, in the context of the model developed here, a continuous change in the polymer density (free volume) is necessary.

The methodology adopted in this work is summarized as follows. First, the radially varying polymer segment density distribution surrounding a single inclusion in an unbounded polymer matrix is approximated using de Gennes's self-consistent mean-field theory. Then the varying segment density is linked to the penetrant diffusivity, using the Cohen-Turnbull free-volume theory, as proposed by Merkel *et al.* Finally, the penetrant concentration disturbances prevailing in a dilute, random distribution of inclusions are averaged to approximate the effective penetrant diffusivity for the composite.

A tractable analytical expression for the radial polymer segment density is obtained from a self-consistent mean-field model, with the so-called ground-state approximation and a flat interface [11]. With a repulsive interaction between the polymer segments and the solid, the segment concentration is [11]

$$c(r) = c_\infty \tanh^2[(r-a)/\xi] + O(\xi/a), \tag{2}$$

where c_∞ is the bulk concentration, and $\xi = l/\sqrt{3\upsilon c_\infty}$ is the polymer correlation length, with l the segment length and υ the excluded volume (per segment).

Note that the mean-field potential that underlies Eq. (2) is proportional to the segment density, and in this sense, it is appropriate for semidilute solutions. However, because correlations are neglected, the theory predicts the incorrect segment-concentration dependence of the correlation length [11]. For concentrated solutions and melts, screening of the excluded-volume interactions may be invoked to neglect correlations. However, in this case, the mean-field potential should have a much stronger (nonlinear) dependence on the segment concentration. Based on these shortcomings, it must be emphasized that the primary role of Eq. (2) here is to provide a simple (two-parameter) model that exhibits a monotonic change in the segment density over a characteristic length ξ.

References connecting ξ to υ and c_∞ below serve to establish that the parameters inferred from experiments provide a qualitative interpretation of reality. Note that the correlation length inferred by fitting the model to the experiments of Merkel *et al.* with silica embedded in PMP is $\xi \approx 0.8$ nm. This is of the expected order of magnitude, and because it is small compared to the inclusion radius ($a \sim 6$ nm), the neglect of surface curvature is reasonably justified.

The Cohen-Turnbull statistical mechanical theory [7] yields a penetrant diffusion coefficient

$$D = A \exp(-\gamma \upsilon_m / \upsilon_f), \tag{3}$$

where A and γ are constants, υ_m is the minimum free volume required for a penetrant molecule to escape its cage of neighboring atoms, and hence undergo diffusive migration, and υ_f is the available free volume per volume occupying element. For simplicity, each atom is assumed to occupy, on average, a volume υ_0, where $\upsilon_0^{1/3}$ is of the order of a covalent bond length ($\approx$1.5 Å). By considering the total volume, which comprises the sum of free and occupied volume, it follows that $\upsilon_f = \upsilon_0[m_1/(\upsilon_0 n_1 \rho) - 1]$, where m_1 is the mass of a monomer (repeat unit), n_1 is the number of atoms per monomer, and ρ is the polymer (mass) density.

It is convenient to introduce a segment volume fraction $\phi = cl^3$, which, by conservation of chain contour length and mass, can be written as $\phi = (\rho/m_1) l_1 l^2$, where l_1 is the length of a monomer. It follows that

$$D = D^\infty \exp\left[-\frac{\upsilon_m^* \phi^* (\phi - \phi_\infty)}{(1-\phi^*\phi)(1-\phi^*\phi_\infty)} \right], \tag{4}$$

where $\phi^* = n_1 \upsilon_0 / (l_1 l^2)$ and $\upsilon_m^* = \gamma \upsilon_m / \upsilon_0$ are dimensionless parameters that reflect the prevailing atomic and molecular geometry.

Setting the bulk polymer volume fraction $\phi_\infty = c_\infty l^3 \approx 1$ and $\upsilon \approx l^3$, it follows that $l^2 \approx m_1/(l_1\rho)$, $\xi \approx l/\sqrt{3}$, and $\phi^* \approx n_1 \upsilon_0 \rho / m_1$. Under these conditions, $1 - \phi^*$ is the fractional free volume of the bulk polymer, and the (maximum) diffusivity at the inclusion-polymer interface becomes

$$D(r=a) \approx D^\infty \exp[\upsilon_m^* \phi^* / (1-\phi^*)]. \tag{5}$$

Clearly, the diffusivity at the interface can be much larger than in the bulk when $\phi^* < 1$ and $\upsilon_m^* < 10$. Note that reverse selectivity prevails because the diffusivity de-

creases continuously with increasing radial distance from the inclusion-polymer interface [12].

Consider, for example, PMP, for which $n_1 = 15$, $m_1 = 81\ \mathrm{g\,mol^{-1}}$, $l_1 \approx 3$ Å, and $\rho \approx 840\ \mathrm{kg\,m^{-3}}$ [2]. These give $l \approx 0.73$ nm and $\xi \approx 0.42$ nm, so with $1 - \phi^* = 0.22$ [3], it follows that $v_0^{1/3} \approx 2.0$ Å and $v_f^{1/3} \approx 1.3$ Å. The same values of v_0 and v_f emerge for poly(p-trimethylsilyl styrene, another highly permeable glass forming polymer.

With a statistically homogeneous microstructure, the average diffusive flux can be expressed as a volume average

$$\langle \boldsymbol{j} \rangle = V^{-1} \int_V \boldsymbol{j} dV, \tag{6}$$

where the integration is over the discrete (inclusion) and continuous (polymer) phases of an elementary volume V. The local diffusive flux is $\boldsymbol{j} = -D\boldsymbol{\nabla} n$, where n is the penetrant concentration. Under steady conditions, conservation demands $\boldsymbol{\nabla} \cdot (D\boldsymbol{\nabla} n) = 0$, with a no-flux boundary condition at $r = a$, a vanishing disturbance as $r \to \infty$, and $D(r)$ from Eqs. (2) and (4). When the volume fraction $\phi_p = n_p(4/3)\pi a^3 \ll 1$, the average flux is [13]

$$\langle \boldsymbol{j} \rangle \approx -D^\infty \langle \boldsymbol{\nabla} n \rangle + 3\phi_p (B/a^3) D^\infty \langle \boldsymbol{\nabla} n \rangle + O(\phi_p^2), \tag{7}$$

where $\langle \boldsymbol{\nabla} n \rangle$ is the average concentration gradient and B is the dipole strength, i.e., $n \to \langle \boldsymbol{\nabla} n \rangle \cdot \boldsymbol{r} + B \langle \boldsymbol{\nabla} n \rangle \cdot \boldsymbol{r} r^{-3}$ as $r \to \infty$.

The effective diffusivity

$$D^e = D^\infty [1 - 3\phi_p (B/a^3)] + O(\phi_p^2) \tag{8}$$

is presented below with $\phi_\infty = 1$ and $\phi^* = 0.8$. The two other independent parameters are the scaled correlation length ξ/a and the scaled penetrant size $v_m^* = \gamma v_m / v_0$. Here, the principal influence of v_m^* is to set the diffusion coefficient at the interface: $D(r = a) = D^\infty \exp(4v_m^*)$.

As expected, all values of $v_m^* > 0$ with sufficiently large ξ/a increase the effective diffusivity. Also, because the relative increase in diffusivity depends exponentially on the penetrant size [Eq. (5)], situations with multiple penetrants exhibit reverse selectivity [1,12].

To compare the theory with experiments, Fig. 1 shows the (scaled) effective diffusivity D^e/D^∞ (lines) and measured values of the (scaled) permeability (circles) for $\phi_p = 0.13$. The $O(\phi_p)$ theory (solid lines) neglects particle interactions, so the values are as given by Eq. (7). The dashed lines are an $O(\phi_p^2)$ theory [12], which has elements of a self-consistent mean-field approximation with an explicit correction for interactions between pairs of particles in a statistically homogeneous dispersion [14]. Note that the (single particle) dipole strength and particle concentration both affect two-body interactions. Some of the experimental scatter may be attributed to the variety of filler particles (all embedded in PMP) and, possibly, different penetrants and degrees of particle aggregation [1].

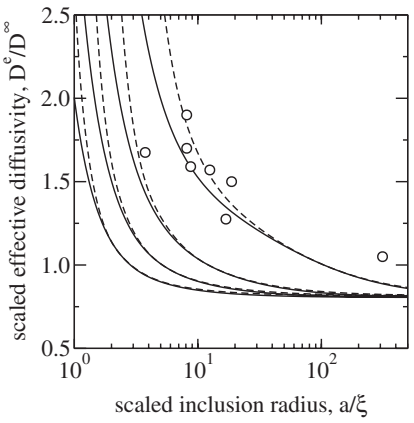

FIG. 1. The scaled effective diffusivity D^e/D^∞ versus the scaled inclusion radius a/ξ with $v_m^* = \gamma v_m / v_0 = 0.1$, 0.2, 0.4, and 1.0 (increasing upward), $\phi^* = 0.8$, and $\phi_p = 0.13$: $O(\phi_p)$ (solid lines); $O(\phi_p^2)$ (dashed lines). The circles are experimental measurements of the permeability enhancement from [1] (reported radii scaled with $\xi = 0.8$ nm).

Nevertheless, with the foregoing approximations, the correlation length inferred by the fit is $\xi = 0.8$ nm (with $\phi^* = 0.8$) and, hence, the segment length $l \approx \sqrt{3}\xi \approx 1.4$ nm. The repeat unit of PMP comprises two bond lengths, so there are about 4.5 monomer units per statistical segment (in the immobilized and compressed chains). As expected, more flexible polymers in solution [e.g., poly(oxyethylene)] have much fewer ($\sim$2) monomer units per statistical segment [15].

Figure 2 shows how the effective diffusivity (with $a = 6.5$ nm) increases with the inclusion volume fraction. The theory is presented with a correlation length $\xi = 0.8$ nm, which was obtained from the fit to data in Fig. 1, so $\xi/a = 0.8/6.5 \approx 0.123$. Despite the experiments extrapolating to

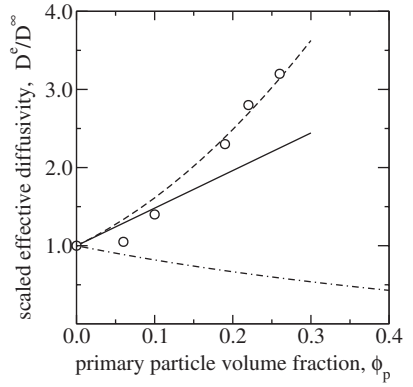

FIG. 2. The scaled effective diffusivity D^e/D^∞ versus the inclusion volume fraction ϕ_p with $v_m^* = \gamma v_m / v_0 = 1.0$, $\phi^* = 0.8$, and $\xi/a = 0.8/6.5 \approx 0.123$: exact $O(\phi_p)$ theory (solid line); approximate $O(\phi_p^2)$ theory (dashed line). The circles are experimental measurements of the permeability enhancement from [1] (with $a = 6.5$ nm). The dash-dotted line is Maxwell's self-consistent theory for impenetrable inclusions and unperturbed (homogeneous) polymer.

a value of $D^e < D^\infty$ as $\phi_p \to 0$, the theoretical and experimental trends are in good agreement. For reference, the dash-dotted line is Maxwell's self-consistent theory for impenetrable inclusions in an unperturbed polymer matrix. It is remarkable, perhaps, that a perturbation extending only $\xi \approx 0.8$ nm from the inclusion surfaces can have such a significant influence on the bulk permeability.

Note that positron annihilation lifetime spectroscopy (PALS) studies [1,2,5] reveal that high-permeability polymers have small *and* large free-volume elements whose radii span the range 0.3–0.60 nm. Furthermore, pulse field gradient (PFG) NMR diffusion studies [3,6] reveal heterogeneity on micron length scales, which, in turn, suggests tortuous interconnected networks of free-volume elements. When silica inclusions are incorporated, PALS indicates a significant increase in the number of large free-volume elements, with a relatively small increase in their size (~10%), while PFG NMR points to increased connectivity of regions with an increased density of free-volume elements.

The conclusions drawn from PFG NMR and PALS are consistent with the theory presented here if the free-volume elements created by the addition of nanoparticles reside at the particle-polymer interface. The interpretation of experiments presented above reveals that the thickness of the depleted layer ($1.5\xi \approx 1.2$ nm) is about twice the radius of the large free-volume elements ascertained by PALS. Therefore, the experimental and theoretical interpretations are compatible if the depleted layer is viewed as a monolayer of free-volume elements.

If the inclusions are well dispersed, then the characteristic size of connected domains would be limited by the inclusion diameter (≈13 nm). While this is considerably larger than the size of the free-volume elements, micron-sized networks (as suggested by PFG NMR) would require primary particles to aggregate. Because the present theory does not account for particle contacts, this shortcoming is, perhaps, one of the more important limitations. Nevertheless, the model accurately describes many of the qualitative and quantitative aspects of the experiments of Merkel *et al.*, so it may still prove to be valuable.

The simplifying approximations adopted in this work are summarized as follows. First, the effective solute diffusivity was compared with experimental measurements of the permeability enhancement, so solubility was assumed to be independent of the inclusion concentration. Next, a mean-field description of the polymer segment density was adopted, with a flat, repulsive interface where the segment-concentration vanishes. Further, the diffusion coefficient was assumed to follow the Cohen-Turnbull formula [Eq. (3)], with the occupied volume proportional to the atomic number density. Finally, the theory applies to a statistically homogeneous dispersion, whereas inclusions may aggregate according to the delicate balance of forces acting between the solvent, polymer, and inclusions during membrane casting.

In conclusion, a (quantitative) theoretical model has been proposed that captures the correct dependence of the bulk (diffusive) permeability of polymeric nanocomposites on the inclusion size and volume fraction. The influence of the nanoinclusions on diffusive selectivity, which is reported elsewhere [12], is also consistent with experiments. Note that the model does not attribute enhanced permeability and selectivity directly to the glassy nature of the dry polymer. Rather, these characteristics arise from a repulsive solvent-mediated interaction between polymer and nanoparticles during membrane casting. It follows that, with a judicious choice of solvent, inclusion surface treatment, and mixing and drying rates, similar effects might be achieved with rubbery polymeric matrices.

This work was supported by the Natural Sciences and Engineering Research Council of Canada (NSERC), through Grant No. 204542, and the Canada Research Chairs program (tier II). The author thanks M. Maric (McGill University) for helpful discussions related to this work.

*Electronic address: reghan.hill@mcgill.ca

[1] T. C. Merkel, B. D. Freeman, R. J. Spontak, Z. He, I. Pinnau, P. Meakin, and A. J. Hill, Science **296**, 519 (2002).
[2] T. C. Merkel, B. D. Freeman, R. J. Spontak, Z. He, I. Pinnau, P. Meakin, and A. J. Hill, Chem. Mater. **15**, 109 (2003).
[3] T. C. Merkel, L. G. Toy, A. L. Andrady, H. Gracz, and E. O. Stejskal, Macromolecules **36**, 353 (2003).
[4] D. Gomes, S. P. Nunes, and J.-V. Peinemann, J. Membr. Sci. **246**, 13 (2005).
[5] P. Winberg, K. DeSitter, C. Dotremont, S. Mullens, I. F. J. Vankelecom, and F. H. J. Maurer, Macromolecules **38**, 3776 (2005).
[6] J. Zhong, G. Lin, W.-Y. Wen, A. A. Jones, S. Kelman, and B. D. Freeman, Macromolecules **38**, 3754 (2005).
[7] M. H. Cohen and D. Turnbull, J. Chem. Phys. **31**, 1164 (1959).
[8] A. Bansal, H. Yang, C. Li, K. Cho, B. C. Benicewicz, S. K. Kumar, and L. S. Schadler, Nat. Mater. **4**, 693 (2005).
[9] S. Asakura and F. Oosawa, J. Chem. Phys. **22**, 1255 (1954).
[10] H. Hervet, L. Léger, and F. Rondelez, Phys. Rev. Lett. **42**, 1681 (1979).
[11] P. G. de Gennes, *Scaling Concepts in Polymer Physics* (Cornell University Press, Ithaca, 1979).
[12] R. J. Hill, Ind. Eng. Chem. Res. (to be published).
[13] R. J. Hill, J. Fluid Mech. **551**, 405 (2006).
[14] D. J. Jeffrey, Proc. R. Soc. A **335**, 355 (1973).
[15] W. B. Russel, D. A. Saville, and W. R. Schowalter, *Colloidal Dispersions* (Cambridge University Press, Cambridge, 1989), p. 168.